

## Energetic Nitrogen-Rich Cu(II) and Cd(II) 5,5'-Azobis(tetrazolate) Complexes

Guo-Hong Tao, Brendan Twamley, and Jean'ne M. Shreeve\*

Department of Chemistry, University of Idaho, Moscow, Idaho, 83844-2343

Received July 27, 2009

Copper(II) and cadmium(II) complexes of 5,5'-azobis(tetrazolate) (ABT) were synthesized at ambient temperature. The anhydrous copper(II) and cadmium(II) salts (**1**) and (**3**) are very impact sensitive. The energetic copper(II) and cadmium(II) ABT coordination complexes, tetraammine copper 5,5'-azobis(tetrazolate) dihydrate [Cu(NH<sub>3</sub>)<sub>4</sub>]-ABT(H<sub>2</sub>O)<sub>2</sub> (**2**) and diammine dihydrate cadmium 5,5'-azobis(tetrazolate) [Cd(NH<sub>3</sub>)<sub>2</sub>(H<sub>2</sub>O)<sub>2</sub>]ABT (**4**) were prepared and then structured by single crystal X-ray diffraction. Their vibrational spectra (IR) were measured and compared with the calculated frequencies. Thermal stabilities were obtained from differential scanning calorimetry measurements and sensitivity toward impact was determined by BAM standards. The energies of combustion of **2** and **4** were based on oxygen bomb calorimetry values and were used to calculate the corresponding heats of formation.

### Introduction

Nitrogen-rich materials combine several advantages such as smokeless combustion, high heats of formation, high propulsive power, and high specific impulse when they are serving as propellants or pyrotechnics.<sup>1</sup> The 5,5'-azobis(tetrazolate) dianion (C<sub>2</sub>N<sub>10</sub><sup>2-</sup>, ABT) is a fascinating component in the construction of high energy density materials (HEDM) because of its extremely high nitrogen content (85.4%). Recently, some organic ABT salts have been prepared and tested as potential materials for modifying the combustion rates of rocket propellants, as gas generators for airbags, and as explosive materials.<sup>2</sup>

The sodium salt (Na<sub>2</sub>ABT) is the most readily accessible ABT salt and is most frequently used as starting material to prepare other ABT salts.<sup>3</sup> Heavy metal Tl and Pb salts of ABT (Tl<sub>2</sub>ABT, Pb<sub>2</sub>(OH)<sub>2</sub>ABT) have been used as initiators.<sup>4</sup> In addition, some alkali, alkaline earth, and rare earth metal ABT salts have also been prepared.<sup>5</sup> However, there are only these few reports available concerning metal ABT salts, and there is a lack of information about the properties of the metal complexes containing the ABT structure. The possible reason is that most anhydrous metal ABT salts, even Na<sub>2</sub>ABT and K<sub>2</sub>ABT, are too shock sensitive and thermally unstable to be manipulated readily.<sup>5</sup>

The various safety properties of novel energetic materials (including sensitivity toward heat, shock, friction, and electrostatic discharge, vapor pressure, vapor toxicity, and decomposition products, etc.), which are closely related to handling, transportation, and utilization, become at least as important as their better energetic characteristics.<sup>6</sup> Although anhydrous metal ABT salts are very sensitive, it is worthwhile to learn more about metal ABT salts because the ABT dianion possesses excellent energetic properties compared with other tetrazole derivatives.<sup>7</sup> The problem is how to lower the sensitivity of the metal ABT salts while concomitantly maintaining

\*To whom correspondence should be addressed. E-mail: jshreeve@uidaho.edu.

(1) (a) Singh, R. P.; Verma, R. D.; Meshri, D. T.; Shreeve, J. M. *Angew. Chem., Int. Ed.* **2006**, *45*, 3584–3601. (b) Christe, K. O.; Wilson, W. W.; Sheehy, J. A.; Boatz, J. A. *Angew. Chem., Int. Ed.* **1999**, *38*, 2004–2009. (c) Chavez, D. E.; Hiskey, M. A.; Gilardi, R. D. *Angew. Chem., Int. Ed.* **2000**, *39*, 1791–1793. (d) Haiges, R.; Boatz, J. A.; Schneider, S.; Schroer, T.; Yousufuddin, M.; Christe, K. O. *Angew. Chem., Int. Ed.* **2004**, *43*, 3148–3152. (e) Huynh, M. H. V.; Hiskey, M. A.; Chavez, D. E.; Naud, D. L.; Gilardi, R. D. *J. Am. Chem. Soc.* **2005**, *127*, 12537–12543. (f) Klapötke, T. M.; Krumm, B.; Scherr, M.; Haiges, R.; Christe, K. O. *Angew. Chem., Int. Ed.* **2007**, *46*, 8686–8690. (g) Abe, T.; Tao, G. H.; Joo, Y.; Huang, Y.; Twamley, B.; Shreeve, J. M. *Angew. Chem., Int. Ed.* **2008**, *47*, 7087–7090. (h) Klapötke, T. M.; Stierstorfer, J. *J. Am. Chem. Soc.* **2009**, *131*, 1122–1134. (i) Zhao, H.; Qu, Z. R.; Ye, H. Y.; Xiong, R. G. *Chem. Soc. Rev.* **2008**, *37*, 84–100. (j) Xiong, R. G.; Xue, X.; Zhao, H.; You, X. Z.; Abrahams, B. F.; Xue, Z. *Angew. Chem., Int. Ed.* **2002**, *41*, 3800–3803.

(2) (a) Hiskey, M. A.; Goldman, N.; Stine, J. R. *J. Energ. Mater.* **1998**, *16*, 119–127. (b) Schmid, H.; Eisenreich, N. *Propellants, Explos. Pyrotech.* **2000**, *25*, 230–235. (c) Hammerl, A.; Klapötke, T. M.; Nöth, H.; Warchhold, M.; Holl, G.; Kaiser, M.; Ticmanis, U. *Inorg. Chem.* **2001**, *40*, 3570–3575. (d) Hammerl, A.; Holl, G.; Kaiser, M.; Klapötke, T. M.; Piotrowski, H. *Z. Anorg. Allg. Chem.* **2003**, *629*, 2117–2121. (e) Sivabalan, R.; Talawar, M. B.; Senthilkumar, N.; Kavitha, B.; Asthana, S. N. *J. Therm. Anal. Calorim.* **2004**, *78*, 781–792. (f) Hammerl, A.; Hiskey, M. A.; Holl, G.; Klapötke, T. M.; Polborn, K.; Stierstorfer, J.; Weigand, J. *J. Chem. Mater.* **2005**, *17*, 3784–3793. (g) Ye, C. F.; Xiao, J. C.; Twamley, B.; Shreeve, J. M. *Chem. Commun.* **2005**, 2750–2752. (h) Klapötke, T. M.; Sabaté, C. M. *Chem. Mater.* **2008**, *20*, 1750–1763.

(3) (a) Thiele, J. *Justus Liebigs Ann. Chem.* **1898**, *303*, 57–75. (b) Singh, G.; Prajapati, R.; Frohlich, R. *J. Hazard. Mater.* **2005**, *118*, 75–78.

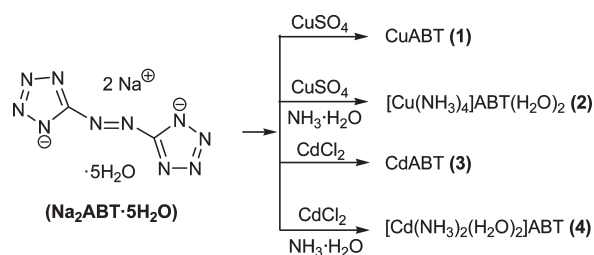
(4) (a) Chaudhri, M. M. *Nature* **1976**, *263*, 121–122. (b) Spear, R. J.; Elischer, P. P. *Aust. J. Chem.* **1982**, *35*, 1–13. (c) Mohan, V. K.; Tang, T. B. *J. Chem. Phys.* **1983**, *79*, 4271–4278.

(5) (a) Hammerl, A.; Holl, G.; Klapötke, T. M.; Mayer, P.; Nöth, H.; Piotrowski, H.; Warchhold, M. *Eur. J. Inorg. Chem.* **2002**, 834–845. (b) Jiao, B. J.; Chen, S. P.; Zhao, F. Q.; Hu, R. Z.; Gao, S. L. *J. Hazard. Mater.* **2007**, *142*, 550–554.

(6) (a) Tao, G. H.; Guo, Y.; Joo, Y.; Twamley, B.; Shreeve, J. M. *J. Mater. Chem.* **2008**, *18*, 5524–5530. (b) Tao, G. H.; Twamley, B.; Shreeve, J. M. *J. Mater. Chem.* **2009**, *19*, 5850–5854. (c) Tao, G. H.; Huang, Y.; Boatz, J. A.; Shreeve, J. M. *Chem.—Eur. J.* **2008**, *14*, 11167–11173.

(7) Steinhauser, G.; Klapötke, T. M. *Angew. Chem., Int. Ed.* **2008**, *47*, 2–20.

Scheme 1. Preparation of Nitrogen-Rich Metal ABT Complexes



their energetic characteristics. On the basis of environmental concerns, the Cu(II) cation was selected as a less toxic metal ion when compared with Ba(II), Pb(II), and Hg(II) in the search for new clean metal-containing energetic materials.<sup>7,8</sup> Here we report structurally characterized transition metal ABT coordination complexes and their energetic properties.

## Results and Discussion

**Synthesis.** Simple metal salts CuABT (**1**) and CdABT (**3**) can be precipitated easily by mixing CuSO<sub>4</sub> or CdCl<sub>2</sub> with sodium 5,5'-azobis(tetrazolate) pentahydrate (Na<sub>2</sub>ABT·5H<sub>2</sub>O)<sup>4</sup> in aqueous solution. However, it is difficult to control the rapid reaction rate to obtain crystals. Recrystallization failed because the green or yellow precipitates are insoluble in water, alcohol, CDCl<sub>3</sub>, and dimethylsulfoxide (DMSO). Just as is the case with other anhydrous metal ABT salts, these simple transition metal ABT salts are too sensitive to be handled safely.<sup>8</sup> Compound **1** detonated one time when touched by a plastic spatula. Attempts to get the IR spectra of **1** and **3** failed. When ~2 mg of **1** or **3** were ground with ~150 mg KBr, the sample exploded.

To obtain relatively stable and safe ABT complexes and to enhance the number of nitrogen atoms by replacing the water of coordination, ammonia was selected as a suitable ligand and stabilizer. Attempts to obtain the crystals by mixing the CuSO<sub>4</sub> or CdCl<sub>2</sub> ammonia solution with Na<sub>2</sub>ABT water solution led to the syntheses of **2** and **4** (Scheme 1). Compound **2**[Cu(NH<sub>3</sub>)<sub>4</sub>]ABT(H<sub>2</sub>O)<sub>2</sub> was obtained by slow diffusion of CuSO<sub>4</sub>·5H<sub>2</sub>O and Na<sub>2</sub>ABT·5H<sub>2</sub>O in concentrated ammonia solution. After the mixture remained overnight at ambient temperature, green needle crystals were found. Compound [Cd(NH<sub>3</sub>)<sub>2</sub>(H<sub>2</sub>O)<sub>2</sub>]ABT (**4**) was obtained from CdCl<sub>2</sub>·2.5H<sub>2</sub>O and Na<sub>2</sub>ABT·5H<sub>2</sub>O in condensed ammonia solution by the same method. Yellow needle crystals were obtained after 2 days.

**Vibrational Spectroscopy.** To obtain a better understanding of the ABT dianion, the molecular orbital and IR absorption frequency analyses based on the optimized structure were carried out using B3LYP functional analyses with the 6-31+G\* basis set.<sup>9</sup> The optimized structure was characterized to be true local energy minima on the potential energy surface without imaginary frequency. The highest occupied molecular orbitals (HOMOs) and lowest unoccupied molecular orbitals

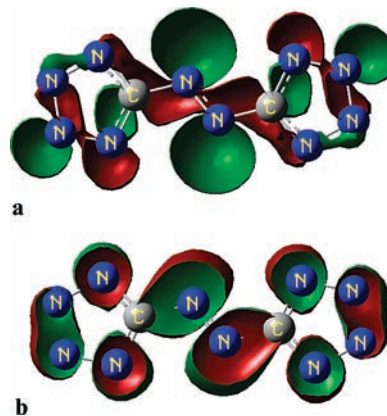


Figure 1. HOMO (a) and LUMO (b) of ABT dianion.

(LUMOs) of the ABT dianion are shown in Figure 1. In the HOMO, the N=N double bond of the azo group may form a large  $\pi$  orbital with the two tetrazolate rings. Another two  $\pi$  orbitals lie across the three nitrogen atoms in the tetrazolate rings. These delocalized bonding orbitals show that the ABT dianion has a strong conjugated effect.

The calculated and the experimental IR data are summarized in Table 1. The calculated IR data can be assigned to four kinds of stretching or bending modes: symmetric or asymmetric stretching ( $\nu_s$ ,  $\nu_{as}$ ), in-plane bending ( $\delta$ ), out-of-plane bending ( $\gamma$ ), and in-plane rocking ( $\omega$ ). In Table 1, only the major infrared frequencies of the ABT dianion are given. Most of them arise from stretching or bending of the tetrazolate rings. As a comparison, all the major frequencies were found at the same region as the experimental IR spectra of **2** and **4**. The stretching and bending frequencies of the N=N double bond were calculated to be 1544 cm<sup>-1</sup> and 911 cm<sup>-1</sup>, respectively, with zero IR intensities. There were no bands observed near these two positions in the experimental IR spectra (see Supporting Information).

In the IR spectra, both **2** and **4** exhibit two intense bands. They were observed centered at 1392 cm<sup>-1</sup>, 734 cm<sup>-1</sup> in **2** and 1404 cm<sup>-1</sup>, 748 cm<sup>-1</sup> in **4**. The two bands are assigned to the asymmetric N=C=N stretching mode of the ring and C-N(=N) stretching mode of the azo group, respectively. The appearance of these two characteristic bands implies the existence of the ABT dianion.<sup>5</sup> Moreover, some characteristic bands arise from the NH<sub>3</sub> ligand and the water. The IR spectrum of **2** show a weak broadband within the range 3350–3250 cm<sup>-1</sup> corresponding to  $\nu(\text{O-H})$ . The low value reveals that the OH group is involved in intermolecular hydrogen bonding. Three different band regions of the main NH<sub>3</sub> modes can be also distinguished. They are assigned as  $\nu_{as}(\text{N-H})$  (3345 cm<sup>-1</sup>),  $\nu_s(\text{N-H})$  (3246 cm<sup>-1</sup>), and  $\delta_{as}(\text{H-N-H})$  (1616 cm<sup>-1</sup>). The  $\nu_{as}(\text{N-H})$  and  $\nu_s(\text{N-H})$  frequencies are shifted to lower wave numbers compared to gaseous NH<sub>3</sub> ( $\nu_{as}(\text{N-H}) = 3414$  cm<sup>-1</sup>,  $\nu_s(\text{N-H}) = 3336$  cm<sup>-1</sup>)<sup>10</sup> because of the coordination effect of NH<sub>3</sub> with the central metal. In the IR spectrum of **4**, The stretching modes  $\nu(\text{O-H})$  are found at 3580 cm<sup>-1</sup> and 3496 cm<sup>-1</sup> because of the two water molecules coordinated with Cd(II). The three characteristic bands of NH<sub>3</sub>

(8) (a) Huynh, M. H. V.; Hiskey, M. A.; Meyer, T. J.; Wetzler, M. *Proc. Natl. Acad. Sci. U.S.A.* **2006**, *103*, 5409–5412. (b) Huynh, M. H. V.; Coburn, M. D.; Meyer, T. J.; Wetzler, M. *Proc. Natl. Acad. Sci. U.S.A.* **2006**, *103*, 10322–10327.

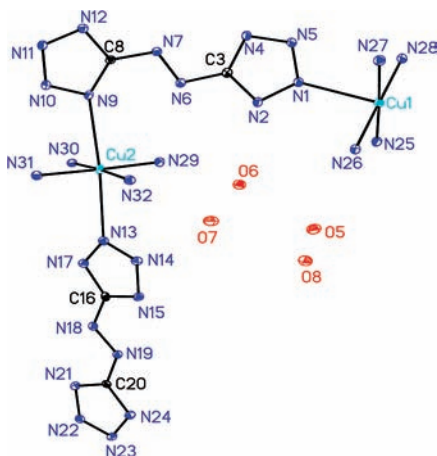
(9) Parr, R. G.; Yang, W. *Density Functional Theory of Atoms and Molecules*; Oxford University Press: New York, 1989.

(10) Fujita, J.; Nakamoto, K.; Kobayashi, M. *J. Am. Chem. Soc.* **1956**, *78*, 3295–3297.

**Table 1.** Calculated IR Data for the ABT Dianion and Experimental IR Data for **2** and **4**

mode assignment <sup>a</sup>	$\nu_{\text{calc}}$ (cm <sup>-1</sup> ) <sup>b</sup>	IR intensity <sup>c</sup>	$\nu_{\text{ex}}$ in <b>2</b> (cm <sup>-1</sup> ) <sup>d</sup>	$\nu_{\text{ex}}$ in <b>4</b> (cm <sup>-1</sup> ) <sup>d</sup>
$\nu_{\text{as}}$	1387	72.9	1392 s	1404 s
$\nu_{\text{s}}$	1213	72.5	1236 m	1213 m
$\nu_{\text{as}}$	1188	19.9	1196 m	1189 s
$\delta$	1076	1.7	1080 w	1072 m
$\nu_{\text{as}}$	1043	25.1	1056 w	1051 m
$\nu_{\text{as}}$	1033	58.8	1038 w	1028 m
$\gamma$	791	4.6	771 m	768 s
$\nu_{\text{as}}$	736	96.4	734 s	748 s
$\omega$	557	20.9	558 m	572 m

<sup>a</sup> Approximate description of vibrational modes:  $\nu_{\text{s}}$ ,  $\nu_{\text{as}}$  = symmetric, asymmetric stretching,  $\delta$  = in-plane bending,  $\gamma$  = out-of-plane bending,  $\omega$  = in-plane rocking. <sup>b</sup> Calculated frequencies. <sup>c</sup> Calculated intensities. <sup>d</sup> Experimental frequencies; qualitative observed intensities.

**Figure 2.** Fragment of the framework in **2** viewed in the direction of 2D planes.

were observed at 3365 cm<sup>-1</sup> ( $\nu_{\text{as}}(\text{N-H})$ ), 3278 cm<sup>-1</sup> ( $\nu_{\text{s}}(\text{N-H})$ ), and 1594 cm<sup>-1</sup> ( $\delta_{\text{as}}(\text{H-N-H})$ ). Compared with the corresponding bands in the spectrum **2**,  $\nu_{\text{as}}(\text{N-H})$  and  $\nu_{\text{s}}(\text{N-H})$  are shifted to higher frequencies, while  $\delta_{\text{as}}(\text{H-N-H})$  shifts to lower frequencies. It is supposed that this occurs because the change of ligand affects the stretching of the N-H bond and the deformation of the angle H-N-H. Experimental IR spectra for **2** and **4** are given in the Supporting Information.

**Crystal Structures.** Single-crystal X-ray analysis of complex **2** shows that it is a two-dimensional coordination inorganic-organic hybrid with bridging ABT ligands. The structure is shown in Figure 2, and crystallographic data are summarized in Table 2. Selected bond distances and angles are given in Table 3. This compound crystallizes in the space group *Pna*2(1) by analysis of systematic absences. The ABT dianion displays delocalization of the negative charge because of bond homogenization (reference bond lengths: C-N, 1.47 Å; N=N, 1.24 Å, and N-N, 1.47 Å). The two independent Cu(II) ions are six-coordinated by two N atoms from the ABT dianion (Cu2-N9 2.526(2) Å, Cu2-N13 2.469(2) Å) and by four N atoms from the coordinated ammonia molecules in the equatorial positions (Cu2-N29 2.025(2) Å, Cu2-N31 2.032(2) Å, Cu2-N32 2.049(2) Å, Cu2-N30 2.051(2) Å). The axial Cu-N bonds are about 0.4–0.5 Å longer than the four basically equivalent equatorial

**Table 2.** X-ray Data and Parameters

	<b>2</b>	<b>4</b>
crystal empirical formula	C <sub>4</sub> H <sub>32</sub> Cu <sub>2</sub> N <sub>28</sub> O <sub>4</sub>	C <sub>5</sub> H <sub>10</sub> CdN <sub>12</sub> O <sub>2</sub>
formula weight	663.66	346.62
<i>T</i> /K	90(2)	90(2)
$\lambda(\text{Mo K}\alpha)/\text{\AA}$	0.71073	0.71073
crystal system	orthorhombic	monoclinic
space group	<i>Pna</i> 2(1)	<i>C</i> 2/ <i>n</i>
<i>a</i> /Å	31.5983(9)	7.2379(5)
<i>b</i> /Å	6.9132(2)	13.6844(10)
<i>c</i> /Å	11.6400(3)	22.2997(16)
$\alpha$	90°	90°
$\beta$	90°	99.1460(10)°
$\gamma$	90°	90°
<i>V</i> /Å <sup>3</sup>	2542.70(12)	2180.6(3)
<i>Z</i>	4	8
<i>d</i> <sub>c</sub> /g·cm <sup>-3</sup>	1.734	2.112
$\mu/\text{mm}^{-1}$	1.747	2.021
<i>F</i> (000)	1368	1360
crystal size/mm	0.57 × 0.08 × 0.06	0.29 × 0.05 × 0.04
crystal color and habit	green needle	yellow needle
reflections collected	37755	15912
unique reflections	5827	1980
<i>R</i> (int)	0.0353	0.0414
parameters	351	92
<i>S</i> on <i>F</i> <sup>2</sup>	1.054	1.038
<i>R</i> 1 ( <i>I</i> > 2 $\sigma$ ( <i>I</i> )) <sup>a</sup>	0.0271	0.0322
<i>wR</i> 2 ( <i>I</i> > 2 $\sigma$ ( <i>I</i> )) <sup>b</sup>	0.0643	0.0834
<i>R</i> 1 (all data)	0.0310	0.0396
<i>wR</i> 2 (all data) <sup>b</sup>	0.0667	0.0886
$\Delta\rho$ min and max/ <i>e</i> ·Å <sup>-3</sup>	0.675 and -0.226	0.866 and -0.722

$$^a R = \sum ||F_o| - |F_c|| / \sum |F_o|. \quad ^b wR = [\sum w(F_o^2 - F_c^2)^2 / \sum w(F_o^2)]^{1/2}.$$

**Table 3.** Selected Bond Lengths [Å] and Angles [deg] for **2**

C(3)–N(2)	1.332(3)	Cu(2)–N(29)	2.025(2)
C(3)–N(4)	1.336(3)	Cu(2)–N(31)	2.032(2)
C(3)–N(6)	1.407(3)	Cu(2)–N(32)	2.049(2)
C(8)–N(9)	1.337(3)	Cu(2)–N(30)	2.051(2)
C(8)–N(12)	1.341(3)	Cu(2)–N(13)	2.469(2)
C(8)–N(7)	1.405(3)	Cu(2)–N(9)	2.526(2)
N(1)–N(5)	1.322(3)	N(29)–Cu(2)–N(31)	178.34(9)
N(1)–N(2)	1.344(3)	N(29)–Cu(2)–N(32)	91.44(8)
N(4)–N(5)	1.346(3)	N(31)–Cu(2)–N(32)	89.35(8)
N(6)–N(7)	1.263(3)	N(29)–Cu(2)–N(30)	88.71(9)
N(9)–N(10)	1.341(3)	N(31)–Cu(2)–N(30)	90.58(9)
N(10)–N(11)	1.332(3)	N(32)–Cu(2)–N(30)	176.72(9)
N(11)–N(12)	1.339(3)	N(13)–Cu(2)–N(9)	175.37(7)

Cu–N bonds. This distorted lengthening Cu(II) center octahedron can be attributed to the Jahn–Teller effect. From Figure 1, it is seen that the electronic density of the HOMO at N9 and N13 atoms is relatively high. It is easy to understand the coordination bond formation between these two N atoms and the copper ion because the latter still has unoccupied 3d orbitals. The types of the bonding orbitals at these two places are different. This causes small differences in the bonds between the Cu and the two tetrazolate rings. (Cu2–N9 2.526(2) Å > Cu2–N13 2.469(2) Å) The ABT dianion serves to bridge two adjacent Cu(II) centers to form a planar dimer. The four water molecules occupy the cavities.

In Figure 3 is depicted the double-layered packing structure of **2** viewed along the *b* axis. Compound **2** was refined as a racemic twin as it crystallizes in a chiral space group. The twin units are zigzag arranged and connected to each other by  $\mu$ -ABT bridges to form a two-dimensional network within the *ac* plane. All of the four water molecules present in the chemical formula are waters of crystallization localized inside the network and linked to the molecular skeleton by hydrogen bonding. Each water

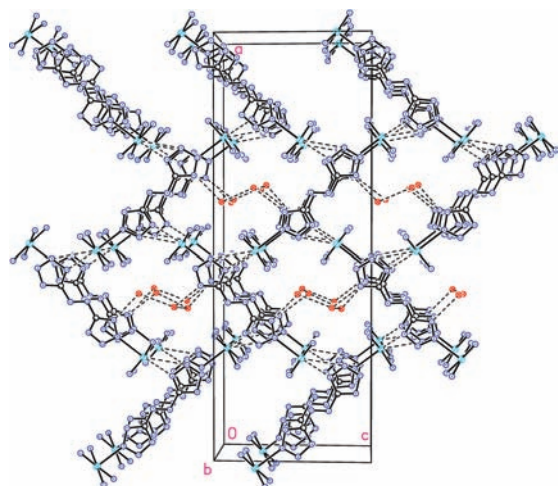


**Figure 3.** Packing diagram of **2** viewed down the *b*-axis. Unit cell indicated and dashed lines represent hydrogen bonding.

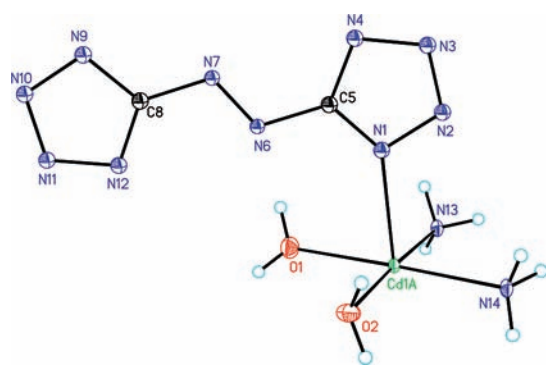


**Figure 4.** Perspective view of the network structure of **4**.

molecule forms moderate hydrogen bonds to the ABT dianions via the nitrogen atoms on the tetrazolate rings ( $O(6)-H(6A)\cdots N(2)$  2.781(3) Å) and also via the ammonia ligands ( $N(29)-H(29B)\cdots O(6)$ , 3.153(3) Å). Each water molecule also forms hydrogen bonds to two other water molecules ( $O(5)-H(5B)\cdots O(8)$  2.774(3) Å,  $O(6)-H(6B)\cdots O(5)$  2.778(3) Å) (see Supporting Information).

Complex **4** crystallizes in a space group  $C2/n$  (Figure 4). In the structure of **4**, the Cd(II) cation is coordinated with two tetrazolate nitrogen atoms of the ABT dianion ( $Cd(1A)-N(1)$  2.422(3) Å,  $Cd(1A)-N(9)$  #1 2.470(3) Å; #1 =  $-x, y + 1/2, -z + 1/2$  symmetry transformation) (Table 4). The coordination geometry around the central Cd(1A) cation sets on an inversion center. The equatorial plane of the octahedron is occupied by two ammonia ligands in a *cis*-orientation ( $Cd(1A)-N(13)$  2.310(3) Å,  $Cd(1A)-N(14)$  2.333(3) Å) and two water molecules ( $Cd(1A)-O(1)$  2.316(4) Å,  $Cd(1A)-O(2)$  2.361(3) Å).

Compound **4** is an infinite one-dimensional coordination array polymer built from centro-asymmetric mononuclear  $[Cd(NH_3)_2(H_2O)_2]$  units that are linked by ABT bridges. There is no water in the crystal except for the two coordinated water molecules. When viewed down the *a* axis, the remarkable structural feature of **4** is that the fundamental units are linked by ABT bridges to form well-isolated bow-like structure chains that run parallel to the *b* axis (Figure 5). The ABT ligand serves as a mono-chelating ligand and forms a bow-like structure at the

**Table 4.** Selected bond lengths [Å] and angles [deg] for **4**<sup>a</sup>

Cd(1A)–N(13)	2.310(3)	N(4)–C(5)	1.335(5)
Cd(1A)–O(1)	2.316(4)	C(5)–N(6)	1.410(5)
Cd(1A)–N(14)	2.333(3)	N(6)–N(7)	1.265(5)
Cd(1A)–O(2)	2.361(3)	N(13)–Cd(1A)–O(1)	88.98(12)
Cd(1A)–N(1)	2.422(3)	N(13)–Cd(1A)–N(14)	92.79(12)
Cd(1A)–N(9)#1	2.470(3)	O(1)–Cd(1A)–N(14)	178.11(11)
N(1)–C(5)	1.337(5)	N(13)–Cd(1A)–O(2)	177.22(11)
N(1)–N(2)	1.344(5)	O(1)–Cd(1A)–O(2)	93.71(12)
N(2)–N(3)	1.324(5)	N(14)–Cd(1A)–O(2)	84.52(12)
N(3)–N(4)	1.346(5)	N(1)–Cd(1A)–N(9)#1	166.25(11)

<sup>a</sup>Symmetry transformations used to generate equivalent atoms: #1 =  $-x, y + 1/2, -z + 1/2$ .

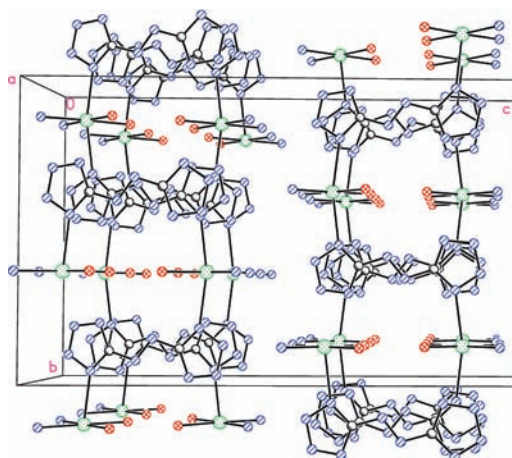


**Figure 5.** Fragment of the framework in **4** viewed along the direction of 1D channels.

1-position nitrogen atoms with the water of the tetrazolate. The two coordinated water molecules present form moderately strong hydrogen bonds molecules on another chain to strengthen the skeleton of the structure. ( $O(1)-H(1B)\cdots O(2)$ #7 3.303(5) Å; #7 =  $-x - 1/2, y + 0, -z + 1/2$  symmetry transformation) (see Supporting Information).

**Physicochemical Properties.** The physicochemical properties of **1–4** are tabulated in Table 5. The densities of **1–4** are from 1.75 to 2.59 g/cm<sup>3</sup>. The simple salts **1** and **3** have higher density. The densities of **2** and **4** are 1.75 and 2.11 g/cm<sup>3</sup>, respectively. These compounds are nitrogen-rich materials with their highest nitrogen content reaching more than 60% (**1**). They have a better oxygen balance than TNT ( $\Omega -74.0\%$ ).<sup>11</sup>

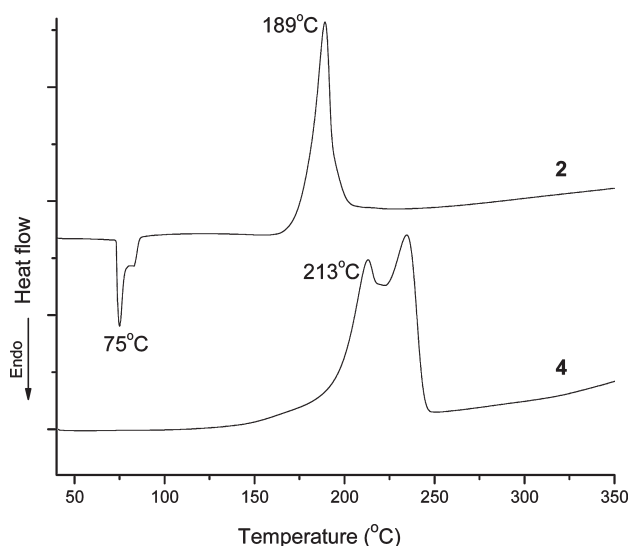
The thermal behavior of the crystals has been investigated using differential scanning calorimetry (DSC). Melting points are not observed in the DSC plots of **1–4**. The decomposition temperatures of **1–4** are in the range of 200 °C based on their onset DSC peaks. Therefore, these metal crystals with the ABT ligand are sufficiently thermally stable to be energetic materials.<sup>8</sup> The simple salts have relatively higher thermal stability than the coordinated complexes which can be most likely attributed to the lack of ligand/water in the structures. For **2**, an endothermic peak is observed at 75 °C corresponding to the loss of two molecules of water of crystallization in addition to the decomposition exotherm (Figure 6). These water molecules disperse among the

(11) Teipel, U. *Energetic Materials*; Wiley-VCH: Weinheim, 2005.

**Table 5.** Physicochemical Properties of **1–4** and Several Typical Metal Energetic Salts

compound	<b>1</b>	<b>2</b>	<b>3</b>	<b>4</b>
MW	227.63	663.66	276.50	346.62
$T_m(^{\circ}\text{C})^a$		75(-H <sub>2</sub> O)		
$T_d(^{\circ}\text{C})^b$	217	189	239	213
$\rho(\text{g}/\text{cm}^3)^c$	2.10	1.75	2.59	2.11
$N(\%)^d$	61.53	59.1	50.66	48.5
$\Omega(\%)^e$	-35.1	-53.0	-28.9	-36.9
IS(J) <sup>f</sup>	< 3	28	< 3	25
$-\Delta_c U(\text{cal}/\text{g})^g$		1261		477
$-\Delta_c H^{\circ}(\text{kJ}/\text{mol})^h$		3482		681
$\Delta_f H^{\circ}(\text{kJ}/\text{mol})^i$		-2979		-1793
$\Delta_f H^{\circ}(\text{kJ}/\text{g})^i$		-4.49		-5.17

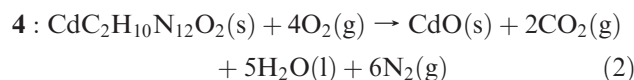
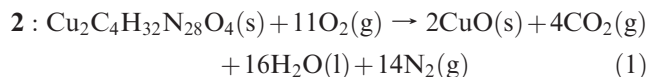
<sup>a</sup> Melting point/DSC endothermic peak. <sup>b</sup> Thermal degradation/DSC exothermic peak. <sup>c</sup> Density, gas pycnometer, 25 °C. <sup>d</sup> Nitrogen content. <sup>e</sup> Oxygen balance, for a compound C<sub>a</sub>H<sub>b</sub>N<sub>c</sub>O<sub>d</sub>M<sub>e</sub>,  $\Omega(\%) = 1600 \cdot [(d - 2a - b/2 - e)/\text{MW}]$  (M, +2 valent metal; MW, molecular weight). <sup>f</sup> Impact sensitivity. <sup>g</sup> Experimental (constant-volume) energy of combustion. <sup>h</sup> Experimental molar enthalpy of combustion. <sup>i</sup> Molar enthalpy of formation.

**Figure 6.** DSC plots of crystals **2** and **4** (heating rate 10 °C/min).

molecules based on weak hydrogen bonding and are easily removed upon heating. Crystal **4** also has two molecules of water in the crystal. However, no endothermic peak was found in the DSC plots of **4**, which occurs because the coordinated water is more strongly bonded than water of crystallization. Thus, this stronger interaction results in the decomposition of **4** at the temperature where water begins to be released.

The experimentally determined constant-volume energies of combustion ( $\Delta_c U$ ) were measured using oxygen bomb calorimetry. The enthalpy of combustion,  $\Delta_c H^{\circ}$ , was calculated from  $\Delta_c U$  and a correction for change in gas volume during combustion was included. The standard enthalpies of formation of **2** and **4**,  $\Delta_f H^{\circ}$ , were back calculated from the heat of combustion on the basis of combustion eq 1 and 2, Hess's Law as applied in thermochemical eqs 3 and 4, and known standard heats of formation for metal oxide, water and carbon dioxide.<sup>12</sup> The combustion energies of **2** and **4**,  $\Delta_c U$ , are -1261 cal/g

and -477 cal/g, respectively. The calculated heats of formation of **2** and **4** are -2979 kJ/mol and -1793 kJ/mol, respectively. These two metal coordination complexes should have relatively thermodynamically stable structures.



$$\Delta_f H^{\circ}(\mathbf{2}, \text{s}) = 2\Delta_f H^{\circ}(\text{CuO}, \text{s}) + 4\Delta_f H^{\circ}(\text{CO}_2, \text{g}) + 16\Delta_f H^{\circ}(\text{H}_2\text{O}, \text{l}) - \Delta_c H^{\circ}(\mathbf{2}, \text{s}) \quad (3)$$

$$\Delta_f H^{\circ}(\mathbf{4}, \text{s}) = \Delta_f H^{\circ}(\text{CdO}, \text{s}) + 2\Delta_f H^{\circ}(\text{CO}_2, \text{g}) + 5\Delta_f H^{\circ}(\text{H}_2\text{O}, \text{l}) - \Delta_c H^{\circ}(\mathbf{4}, \text{s}) \quad (4)$$

The impact sensitivity was determined by the drop hammer test (BAM method).<sup>13</sup> The impact sensitivity of **1** and **3** are both less than 3 J. On the basis of the UN standard,<sup>14</sup> they are classified as impact very sensitive energetic materials. Therefore, **1** and **3** may be used as potential initiators or detonators. The impact sensitivity of **2** and **4** were measured to be 28 and 25 J, respectively. They may be classified as impact sensitive energetic materials. They have lower impact sensitivities than TNT (15 J).<sup>11</sup>

## Conclusion

Transition metal ABT salts were prepared and characterized. Two stable metal coordination complexes with the energetic nitrogen-rich ABT ligand have been studied by single-crystal X-ray analysis and a combination of theoretical calculations and experimental IR analysis. Their physicochemical properties were determined and discussed. Furthermore, they are all impact sensitive/very sensitive energetic materials. The copper ABT salts may be potential "green" energetic materials as gas generators or additives in solid rockets as low-smoke propellants ingredients.

## Experimental Section

**Caution!** The reported compounds are all impact sensitive/very sensitive materials, their friction sensitivities have not been determined. Especially the simple metal ABT salts are very sensitive to light contact with a spatula. Therefore, they should be handled on small scale (< 1 mmol) with extreme care using all of the standard safety precautions such as leather gloves, leather coat, face shields, and ear plugs.

All chemicals were pure analytical grade materials obtained commercially and used as received. Infrared spectra were recorded using KBr pellets for solids on a Biorad Model 3000 FTS spectrometer. The densities of the solids were measured at 25 °C using a Micromeritics Accupyc 1330 gas pycnometer. DSC measurements were performed using a TA

(12) Standard Thermodynamic Properties of Chemical Substances. In *CRC Handbook of Chemistry and Physics, Internet Version 2007*, 87th ed.; Lide, D. R., Ed.; Taylor and Francis: Boca Raton, FL, 2007.

(13) Reichel & Partner GmbH, <http://www.reichel-partner.de/>.

(14) Impact: insensitive > 40 J, less sensitive  $\geq 35$  J, sensitive  $\geq 4$  J, very sensitive  $\leq 3$  J. According to the UN Recommendations on the Transport of Dangerous Goods.

DSCQ10 calorimeter equipped with an autocool accessory and calibrated using indium. The following procedure was used: heating from 40 to 400 °C at 10 °C/min. Elemental analyses (C, H, N) were performed on a CE-440 Elemental Analyzer. Impact sensitivity tests were carried out using a BAM Fallhammer method. The calorimetric measurements were measured using a Parr 1425 semimicro bomb calorimeter equipped with a Parr 1672 calorimetric thermometer. The samples were burned in a 3.2 MPa atmosphere of pure oxygen. Computations were performed by using the Gaussian03 (Revision D.01) suite of programs.<sup>15</sup> Sodium azobis(tetrazolate) pentahydrate was prepared following a literature method.<sup>3</sup>

**X-ray Crystallographic Experimental.** Crystals of compound [Cu(NH<sub>3</sub>)<sub>4</sub>]ABT(H<sub>2</sub>O)<sub>2</sub> (**2**) or [Cd(NH<sub>3</sub>)<sub>2</sub>(H<sub>2</sub>O)<sub>2</sub>]ABT (**4**) were removed from the beaker, a suitable crystal was selected, attached to a glass fiber and data were collected at 90(2) K using a Bruker/Siemens SMART APEX instrument (Mo K $\alpha$  radiation,  $\lambda = 0.71073$  Å) equipped with a Cryocool NeverIce low temperature device. Data were measured using  $\omega$  scans 0.3° per frame for 20 s, and a full sphere of data was collected. A total of 2400 frames were collected with a final resolution of 0.77 Å. Cell parameters were retrieved using SMART<sup>16</sup> software and refined using SAINTPlus<sup>17</sup> on all observed reflections. Data reduction and correction for Lp and decay were performed using the SAINTPlus software. Absorption corrections were applied using SADABS.<sup>18</sup> The structure was solved by direct methods and refined by least-squares method on  $F^2$  using the SHELXTL program package.<sup>19</sup> No decomposition was observed during data collection.

(15) Frisch, M. J.; Trucks, G. W.; Schlegel, H. B.; Scuseria, G. E.; Robb, M. A.; Cheeseman, J. R.; Montgomery, J. A., Jr.; Vreven, T.; Kudin, K. N.; Burant, J. C.; Millam, J. M.; Iyengar, S. S.; Tomasi, J.; Barone, V.; Mennucci, B.; Cossi, M.; Scalmani, G.; Rega, N.; Petersson, G. A.; Nakatsuji, H.; Hada, M.; Ehara, M.; Toyota, K.; Fukuda, R.; Hasegawa, J.; Ishida, M.; Nakajima, T.; Honda, Y.; Kitao, O.; Nakai, H.; Klene, M.; Li, X.; Knox, J. E.; Hratchian, H. P.; Cross, J. B.; Bakken, V.; Adamo, C.; Jaramillo, J.; Gomperts, R.; Stratmann, R. E.; Yazyev, O.; Austin, A. J.; Cammi, R.; Pomelli, C.; Ochterski, J. W.; Ayala, P. Y.; Morokuma, K.; Voth, G. A.; Salvador, P.; Dannenberg, J. J.; Zakrzewski, V. G.; Dapprich, S.; Daniels, A. D.; Strain, M. C.; Farkas, O.; Malick, D. K.; Rabuck, A. D.; Raghavachari, K.; Foresman, J. B.; Ortiz, J. V.; Cui, Q.; Baboul, A. G.; Clifford, S.; Cioslowski, J.; Stefanov, B. B.; Liu, G.; Liashenko, A.; Piskorz, P.; Komaromi, I.; Martin, R. L.; Fox, D. J.; Keith, T.; Al-Laham, M. A.; Peng, C. Y.; Nanayakkara, A.; Challacombe, M.; Gill, P. M. W.; Johnson, B.; Chen, W.; Wong, M. W.; Gonzalez, C.; Pople, J. A. *Gaussian 03*, Revision D.01; Gaussian, Inc.: Wallingford, CT, 2004.

(16) SMART, v. 5.632; Bruker AXS: Madison, WI, 2005.

(17) SAINTPlus, v. 7.23a, *Data Reduction and Correction Program*; Bruker AXS: Madison, WI, 2004.

(18) SADABS, v.2007/4, *an empirical absorption correction program*; Bruker AXS Inc.: Madison, WI, 2007.

(19) Sheldrick, G. M. SHELXTL: v. 6.14, *Structure Determination Software Suite*; Bruker AXS Inc.: Madison, WI, 2004.

**Copper 5,5'-Azobis(tetrazolate) (CuABT) (1).** Twenty-five milligrams (0.1 mmol) of copper sulfate pentahydrate was dissolved in water (5 mL). Then an aqueous solution of sodium 5,5'-azobis(tetrazolate) pentahydrate (30 mg, 0.1 mmol, 10 mL) was slowly added with stirring. A green precipitate was separated and dried in air. Yield: 22 mg (97%). Elemental analysis not successful; the sample exploded.

**Tetraammine Copper 5,5'-Azobis(tetrazolate) Dihydrate ([Cu(NH<sub>3</sub>)<sub>4</sub>]ABT(H<sub>2</sub>O)<sub>2</sub>) (2).** A 50 mg portion (0.2 mmol) of copper sulfate pentahydrate was dissolved in ammonia–water solution (5 mL, 28%–30% NH<sub>3</sub>). Then an aqueous solution of sodium 5,5'-azobis(tetrazolate) pentahydrate (60 mg, 0.2 mmol, 20 mL) was slowly added to form a clear green solution. Green needles [Cu(NH<sub>3</sub>)<sub>4</sub>]ABT(H<sub>2</sub>O)<sub>2</sub> crystallized from the solution overnight. Yield: 61 mg (92%). IR: 3345 s, 3246 m, 3178 m, 2108 w, 1616 m, 1392 s, 1294 m, 1268 m, 1249 m, 1236 m, 1196 m, 1157 w, 1080 w, 1056 w, 1038 w, 771 m, 734 s, 699 m, 558 m. Calcd for C<sub>4</sub>H<sub>32</sub>Cu<sub>2</sub>N<sub>28</sub>O<sub>4</sub> (663.57): C 7.24, H 4.86, N 59.10; found C 7.24, H 4.23, N 58.65.

**Cadmium 5,5'-Azobis(tetrazolate) (CdABT) (3).** Twenty-three milligrams (0.1 mmol) of cadmium chloride hemipentahydrate was dissolved in water (5 mL). Then an aqueous solution of sodium 5,5'-azobis(tetrazolate) pentahydrate (30 mg, 0.1 mmol, 10 mL) was slowly added with stirring. A yellow precipitate was separated and dried in air. Yield: 26 mg (94%). Calcd for C<sub>2</sub>CdN<sub>10</sub> (276.50): C 8.69, N 50.66; found C 8.27, N 50.25.

**Diammine Cadmium 5,5'-Azobis(tetrazolate) Dihydrate ([Cd(NH<sub>3</sub>)<sub>2</sub>(H<sub>2</sub>O)<sub>2</sub>]ABT) (4).** A 46 mg portion (0.2 mmol) of cadmium chloride hemipentahydrate was dissolved in ammonia–water solution (5 mL). Then an aqueous solution of sodium 5,5'-azobis(tetrazolate) pentahydrate (60 mg, 0.2 mmol, 20 mL) was slowly added to form a clear yellow solution. Yellow needles [Cd(NH<sub>3</sub>)<sub>2</sub>(H<sub>2</sub>O)<sub>2</sub>]ABT crystallized from the solution after 2 days. Yield: 60 mg (87%). IR: 3580 m, 3496 m, 3365 s, 3278 m, 2140 w, 1594 m, 1404 s, 1213 m, 1189 s, 1111 w, 1072 m, 1051 m, 1028 m, 768 s, 748 s, 618 m, 572 m. Calcd for C<sub>2</sub>H<sub>10</sub>CdN<sub>12</sub>O<sub>2</sub> (346.59): C 6.93, H 2.91, N 48.50; found C 6.92, H 2.90, N 49.12.

**Acknowledgment.** The authors gratefully acknowledge the support of DTRA (HDTRA1-07-1-0024), NSF (CHE-0315275), and ONR (N00014-06-1-1032). The Bruker (Siemens) SMART APEX diffraction facility was established at the University of Idaho with the assistance of the NSF-EPSCoR program and the M. J. Murdock Charitable Trust, Vancouver, WA, U.S.A.

**Supporting Information Available:** X-ray crystallographic information including the CIF file and IR spectra of **2** and **4**. This material is available free of charge via the Internet at <http://pubs.acs.org>.